Journal of Alzheimer's Disease 34 (2013) 707–725
DOI 10.3233/JAD-121807
IOS Press

Resting State Cortical Electroencephalographic Rhythms in Covert Hepatic Encephalopathy and Alzheimer's Disease

Claudio Babiloni[a,b,*], Fabrizio Vecchio[c], Claudio Del Percio[b], Sara Montagnese[d], Sami Schiff[d], Roberta Lizio[b], Giorgia Chini[e], Gaetano Serviddio[f], Nicola Marzano[g], Andrea Soricelli[g,h], Giovanni B. Frisoni[i], Paolo M. Rossini[b,j] and Piero Amodio[e]
[a]*Department of Molecular Medicine, University of Rome Sapienza, Rome, Italy*
[b]*IRCCS San Raffaele Pisana, Rome, Italy*
[c]*A.Fa.R., Dip. Neurosci. Osp. FBF, Isola Tiberina, Rome, Italy*
[d]*Clinical and Experimental Medicine, University of Padova, Padova, Italy*
[e]*Department of Informatics and Systemistics, University of Rome Sapienza, Rome, Italy*
[f]*Department of Medical and Occupational Sciences, University of Foggia, Foggia, Italy*
[g]*IRCCS "SDN", Naples, Italy*
[h]*Università degli Studi di Napoli Parthenope, Napoli, Italy*
[i]*IRCCS "S. Giovanni di Dio-F.B.F.", Brescia, Italy*
[j]*Departments of Geriatrics, Neurosciences & Orthopedics, Catholic University "Sacro Cuore", Rome, Italy*

Accepted 28 November 2012

Abstract. Patients suffering from prodromal (i.e., amnestic mild cognitive impairment, aMCI) and overt Alzheimer's disease (AD) show abnormal cortical sources of resting state electroencephalographic (EEG) rhythms. Here we tested the hypothesis that these sources show extensive abnormalities in liver cirrhosis (LC) patients with a cognitive impairment due to covert and diffuse hepatic encephalopathy (CHE). EEG activity was recorded in 64 LC (including 21 CHE), 21 aMCI, 21 AD, and 21 cognitively intact (Nold) subjects. EEG rhythms of interest were delta (2–4 Hz), theta (4–8 Hz), alpha 1 (8–10.5 Hz), alpha 2 (10.5–13 Hz), beta 1 (13–20 Hz), and beta 2 (20–30 Hz). EEG cortical sources were estimated by LORETA. Widespread sources of theta (all but frontal), alpha 1 (all but occipital), and alpha 2 (parietal, temporal) rhythms were higher in amplitude in all LC patients than in the Nold subjects. In these LC patients, the activity of central, parietal, and temporal theta sources correlated negatively, and parietal and temporal alpha 2 sources correlated positively with an index of global cognitive status. Finally, widespread theta (all but frontal) and alpha 1 (all but occipital) sources showed higher activity in the sub-group of LC patients with CHE than in the patients with aMCI or AD. These results unveiled the larger spatial-frequency abnormalities of the resting state EEG sources in the CHE compared to the AD condition.

Keywords: Alzheimer's disease, covert hepatic encephalopathy, electroencephalography, hepatic encephalopathy, liver cirrhosis, low resolution brain electromagnetic tomography, mild cognitive impairment, minimal hepatic encephalopathy

INTRODUCTION

Hepatic encephalopathy (HE) is a brain dysfunction caused by liver insufficiency and/or portal-systemic shunting. HE produces a wide spectrum of nonspecific

*Correspondence to: Claudio Babiloni, Ph.D., Department of Molecular Medicine, University of Rome "Sapienza", Rome, Piazzale Aldo Moro, 5, Roma I-00185, Italy. Tel.: +39 06 49910989; Fax: +39 06 49910917; E-mail: claudio.babiloni@uniroma1.it.

ISSN 1387-2877/13/$27.50

neurological and psychiatric manifestations [1]. In its subclinical phase (i.e., no clinically-overt cognitive dysfunction), HE causes a kind of minimal cognitive impairment concerning attention, working memory, psychomotor speed, and visuo-spatial ability detectable by neuropsychological or psychophysical tests, as well as neurophysiological alterations [2]. This condition is called minimal HE (MHE) [3–5]. Approximately 30–80% of patients with cirrhosis may show MHE [2, 6]. MHE is associated with poor quality of life and a high risk of traffic violations and accidents [7, 8]. It is also associated with an increased progression to overt HE (i.e., from confusion to coma).

The severity of HE is graded with the well-known West Haven Criteria; this scale is based on the level of impairment of autonomy, changes in consciousness, intellectual function, behavior, and the dependence on therapy [6]. The West Haven Criteria span from grade 1 (i.e., a poorly reproducible stage of HE in which an observer can detect some patient's negligible symptoms, such as trivial lack of awareness, euphoria or anxiety, shortened attention span, and impaired performance of addition or subtraction) to grade 4 (i.e., coma as unresponsive to verbal or noxious stimuli) on the basis of a structured clinical evaluation and use of standardized items (e.g., Does the patient know which month it is? Does the patient know the day of the week? Can the patient count backward from 10 to 1 without making mistakes or stopping?, etc.). Recently, the term 'covert HE' (CHE) was coined, pooling MHE with West Haven grade I HE [9]. The concept of CHE is more and more used in the literature [10], and we will use it to name these patients in the following.

Several studies have shown that spectral analysis of electroencephalographic (EEG) rhythms in awake subjects at rest (eyes closed) is a low-cost, easy to perform, and widely available neurophysiological approach for the study of HE [8, 11–20]. Indeed, resting state EEG markers are virtually not affected by anxiety for performance, emotional variables, skillfulness, and subjects' social compliance. Furthermore, recording of the resting state EEG rhythms can be repeated countless times in the follow up of patients with liver cirrhosis (LC) to monitor for CHE without the learning effects or the need of cooperation which plague psychometric testing. Finally, resting state EEG rhythms seem to provide (at least at group level) useful markers/end points to evaluate disease progression in subjects with HE.

Previous studies have shown that spectral analysis of resting state EEG rhythms allows a classification of HE subjects in line with clinical severity of the disease [13, 15]. It also allows the detection of CHE [12, 14, 21] and some prediction of the progression to overt HE and liver-related death, at least in patients with advanced liver disease [8]. In particular, mean dominant EEG frequency was significantly "slower" in HE patients compared to healthy controls [18, 20]. In addition, theta (4–8 Hz) and alpha (8–12 Hz) rhythms showed different magnitude in individuals with even CHE compared to healthy controls [18, 19, 22]. Such changes were associated to a remarkable topographical anteriorization of the maximum power density at theta and alpha rhythms from the occipital toward the parietal and central derivations, thus resembling some neural correlates of drowsiness preceding sleep onset [23–26]. In CHE patients, the anteriorization of the dominant theta or alpha rhythms has also been quantified by analytical techniques such as spatiotemporal decomposition, which separated the main components of the EEG and defined their distribution across the scalp [27]. Finally, EEG power density was found to be correlated to psychometric hepatic findings [22, 28]. These findings complement preceding evidence showing that, at group level, cortical sources of resting state eyes-closed cortical EEG rhythms present topographical and frequency differences in healthy normal elderly subjects (Nold) and patients with cognitive impairment [29–32]. When compared to Nold subjects, subjects with amnestic mild cognitive impairment (aMCI; a sort of prodromal AD condition) showed a power density decrease of posterior alpha sources [29–32], whereas AD subjects were characterized by a power density increase of topographically widespread delta and theta sources and a power decrease of posterior alpha sources [29, 33, 34]. In addition, posterior alpha sources had lower power density in AD than in cerebrovascular dementia (CVD) and in Parkinson disease with dementia (PDD), whereas topographically widespread theta rhythms were higher in power density in CVD and PDD than AD subjects [29, 35].

In the present study, we tested the hypothesis of peculiar abnormalities in the spatial distribution and in the frequency bands of the cortical sources of resting state EEG rhythms in patients with CHE when compared to patients with possible prodromal or overt AD. As a novelty, the present study used a validated procedure for the estimation of these cortical sources (i.e., low resolution brain electromagnetic tomography (LORETA)) to directly compare the results obtained in CHE and AD populations. It is expected that both CHE and AD pathologies reflect peculiar abnormalities in the abnormal fluctuation of cortical arousal, which are expected to be reflected by resting state EEG rhythms. The EEG features able to capture these

peculiar abnormalities would be candidate markers to enlighten the neurophysiological mechanisms of action of the drugs for the two pathologies. This is a promising perspective for the development of new drugs and therapy monitoring in AD and CHE patients. Indeed, the present EEG methodological approach has a sufficient spatial and frequency resolution to unveil narrower EEG abnormalities in spatial and frequency domain in AD than in CHE patients. This prediction is based on the notion that at earlier stages of the clinical disease, MCI and AD patients show neurodegenerative processes circumscribed in few brain regions such as hippocampus, enthorinal paleocortex, and posterior neocortex [36]. On the other hand, CHE patients are characterized by effects of blood neurotoxins on widespread brain regions spanning several sub-cortical and cortical structures [37].

The main novelty of the present study is that for the first time the same EEG methodological approach was used in two matched populations with similar cognitive deficits but quite different neuropathologies such as AD and CHE. This is the first exploratory comparison of the spatial-frequency patterns of the cortical sources of resting state cortical EEG rhythms in these two pathological conditions affecting human cognition, beyond the same or similar outcome at mere behavioral/cognitive level.

METHODS

Subjects

We enrolled 64 (28% of females) patients with liver cirrhosis (LC) and 64 (33% of females) cognitively intact age-matched elderly (Nold) subjects as a control group. The mean subjects' age was 58.2 ($\pm$0.9 standard error, SE) years in the LC patients, and 59.5 ($\pm$0.8 SE) years in the Nold subjects. Despite age and gender being comparable ($p > 0.05$), they were used as covariates in the subsequent statistical analysis, to adjust for the slight trend for an excess of women in Nold subjects.

Out of the 64 LC patients, 21 (33% of females; 61.1 ± 2.1 years) were recognized to have CHE on the basis of abnormalities revealed by the psychometric evaluation and/or signs of grade 1 HE on a structured clinical examination performed by a clinician with international experience in HE studies (S.M.). This procedure reflected our daily clinical routine in the framework of an exploratory investigation. To study the peculiar cortical sources of resting state EEG rhythms of the CHE sub-group, we selected the following age- and gender-matched control populations: 21 (33% of females; 61.2 ± 0.8 years) Nold subjects, 21 (33% of females; 63.4 ± 1.2 years) aMCI subjects, and 21 (33% of females; 62.6 ± 1.7 years) AD patients. Analysis of variance (ANOVA) using the factor Group (CHE, Nold, aMCI, AD) for age confirmed the match goodness ($p > 0.5$). Local institutional ethics committees approved the study. All experiments were performed with the informed and overt consent of each participant or caregiver, in line with the Code of Ethics of the World Medical Association (Declaration of Helsinki) and the standards established by the authors' institutional review board.

Diagnostic criteria

The inclusion diagnostic criteria to enroll LC patients were the following: (i) the presence of hepatic stigmata on routine clinical examination, together with biochemical indices of decompensated liver disease (i.e., low serum albumin, high bilirubin, prolonged prothrombin time, low platelet count); (ii) endoscopic or ultrasound signs of portal hypertension, or a history of previous decompensation (ascites, jaundice, bleeding from esophageal varices); (iii) mental or motor disorders including subtle cognitive changes/confusion, deep altered levels of cognitive functioning/consciousness, irritability, tremor, difficulties with coordination.

Exclusion criteria included patients with past disorders that could have negative effects on cerebral functioning such as heart failure, endocrinological diseases, respiratory or renal insufficiency, neuropsychiatric diseases, cerebrovascular diseases, dementia, or epilepsy or those who were taking psychotropic drugs. In this regard, it should be remarked that brain imaging (i.e., magnetic resonance imaging, MRI) was not routinely performed, as it is not required for the diagnosis of HE. MRI was used in a minority of the cases when the CHE patients' history and medical documentation suggested that the cognitive decline might be due to not only LC but also to other comorbidities. In the majority of the cases, the patients' history and medical documentation were directly used to exclude other causes of cognitive decline (note that all enrolled LC patients have received long-term follow ups to exclude major comorbidities). Furthermore, all LC patients underwent EEG recordings to exclude signs of local brain suffer and epilepsy.

The LC patients underwent psychometric evaluation by the porto-hepatic encephalopathy score (PHES), comprising the following procedures: the Trial

Table 1
Mean value (±standard error) of psychometric data in patients with liver cirrhosis (LC) and LC patients with covert hepatic encephalopathy (CHE). The following psychometric tests were considered: Trial Making Test A and Test B, the Symbol Digit Test, the Serial Dotting Test, and the Line Trait Test. The mean Z psychometric score of the above mentioned tests is also reported as a synthetic psychometric index

Psychometric tests	LC Unimpaired	LC CHE
Trail making test part A (s)	50.1 (±3.1)	67.6 (±5.9)
Trail making test part B (s)	150.5 (±14.1)	228 (±31.4)
Symbol digit test items/90 (s)	28.6 (±1.3)	20.7 (±1.6)
Serial dotting test (s)	65.4 (±4.3)	82.1 (±8.1)
Line trait test-time (s)	90.7 (±4.9)	115.2 (±9.2)
Line trait test-errors (errors)	13.9 (±2.6)	20.8 (±6)
Mean Z-score of all the psychometric tests	−0.31 (±0.1)	−1.2 (±0.3)

Table 2
Brodmann areas included in the cortical regions of interest (ROIs) of the present study. LORETA solutions were collapsed in frontal, central, parietal, occipital, temporal, and limbic ROIs

LORETA Brodmann Areas into the Regions of Interest	
Frontal	8, 9, 10, 11, 44, 45, 46, 47
Central	1, 2, 3, 4, 6
Parietal	5, 7, 30, 39, 40, 43
Temporal	20, 21, 22, 37, 38, 41, 42
Occipital	17, 18, 19
Limbic	31, 32, 33, 34, 35, 36

Making Test A and B, the Digit Symbol test, the Serial Dotting, and the Line Trait Test [38, 39]. For each test, age and education- adjusted Z score was calculated. The PHES is the sum of the integer scores of each test computed from the adjusted Z values as follows: score = −3 for $Z \leq -3$, score = −2 for $-3 < Z \leq -2$, score = −1 for $-2 < Z \leq -1$, score = 0 for $-1 < Z < 1$, score = 1 for $Z > 1$. CHE was diagnosed as follows: 1) existence of hepatic cirrhosis, 2) orientation for time and space, 3) alteration of PHES (≤ -4), standardized for the national population [40], 4) exclusion of concurrent disorders that could have negative effects on cerebral functioning (heart failure –NYHA ≥ 2-, endocrinological diseases (in particular, hypothyroidism), respiratory or renal insufficiency, neuropsychiatric diseases, cerebrovascular diseases, dementia, epilepsy, or consumption of psychotropic drugs.

In addition, the mean Z psychometric score (MZPS) of the above mentioned tests was evaluated as a synthetic psychometric index of global cognitive status both for simplicity and to reduce bias due to multiple comparison [40]. Psychometric data for unimpaired LC and CHE patients are summarized in Table 1.

Inclusion and exclusion criteria for aMCI subjects were based on previous seminal reports [41, 42]. Summarizing, the inclusion criteria were as follows: (i) objective memory impairment on neuropsychological evaluation probing cognitive performance in the domains of memory, language, executive function/attention, etc.; (ii) normal activities of daily living as documented by the history and evidence of independent living; and (iii) clinical dementia rating (CDR; [43]) score of 0.5. The exclusion criteria included: (i) mild dementia of the AD type, as diagnosed by standard protocols including NINCDS-ADRDA [44] and DSM-IV; (ii) evidence (including MRI procedures) of concomitant cerebral impairment such as frontotemporal degeneration, cerebrovascular disease as indicated by Hatchinski ischemic score [45], MRI vascular lesions, and reversible cognitive impairment (including depressive pseudo-dementia); (iii) marked fluctuations in cognitive performance compatible with Lewy body dementia and/or features of mixed cognitive impairment including cerebrovascular disease; (iv) evidence of concomitant extra-pyramidal symptoms; (v) clinical and indirect evidence of depression as revealed by the Geriatric Depression Scale (GDS; [46]) scores >14; (vi) other psychiatric diseases, epilepsy, drug addiction, alcohol dependence (as revealed by a psychiatric interview) and use of psychoactive drugs including acetylcholinesterase inhibitors or other drugs enhancing brain cognitive functions; and (vii) current or previous uncontrolled or complicated systemic diseases (including diabetes mellitus) or traumatic brain injuries.

Probable AD was diagnosed according to NINCDS-ADRDA [40] and DSM IV criteria. The recruited AD patients underwent general medical, neurological, neuropsychological, and psychiatric assessments. Patients were rated with a number of standardized diagnostic and severity instruments that included Mini Mental State Evaluation (MMSE, [47]), CDR [43], GDS [46], Hachinski Ischemic Score [45], and Instrumental Activities of Daily Living scale [48]. Neuroimaging diagnostic procedures (MRI) and complete laboratory analyses were carried out to exclude other causes of progressive or reversible dementias, in order to have a clinically homogenous mild AD group. Exclusion criteria included any evidence of (i) frontotemporal dementia, (ii) vascular dementia, diagnosed according to NINDS-AIREN criteria [49], (iii) extra-pyramidal syndromes, (iv) reversible dementias (including pseudodementia of depression); and (v) Lewy body dementia, according to the criteria by McKeith [50].

Finally, the Nold subjects were recruited mostly from non-consanguineous relatives of AD patients. All

Nold subjects underwent physical and neurological examinations as well as cognitive screening (including MMSE). Among them, those affected by chronic systemic illnesses (i.e., diabetes mellitus or organ failure) were excluded, as were subjects receiving psychoactive drugs. The Nold subjects with history of present or previous neurological or psychiatric disease were also excluded. All Nold subjects had a GDS score lower than 14 (no depression).

EEG recordings

EEG data were recorded by specialized clinical units in the recruited subjects at resting state (eyes-closed). The EEG recordings were performed (0.3–70 Hz bandpass) from 19 electrodes positioned according to the International 10–20 System (i.e., Fp1, Fp2, F7, F3, Fz, F4, F8, T3, C3, Cz, C4, T4, T5, P3, Pz, P4, T6, O1, O2). A specific reference electrode was not imposed to the recording clinical units of this study, since preliminary data inspection and EEG source analysis were carried out after EEG data were re-referenced to a common average reference. To monitor eye movements, the horizontal and vertical electrooculogram (0.3–70 Hz bandpass) was also collected. All data were digitized in continuous recording mode (few minutes of EEG; 256 Hz sampling rate). The EEG recordings were performed in the late morning. In order to keep constant the level of vigilance, an experimenter controlled online the subject and the EEG traces to avoid sleep onset.

Preliminary EEG-EOG data analysis

The recorded EEG data were analyzed and segmented off-line in consecutive epochs of 2 s. The EEG epochs with ocular, muscular, and other types of artifact were preliminary identified by a computerized automatic procedure. The EEG epochs with sporadic blinking artifacts (less than 10% of the total) were corrected by an autoregressive method [51]. Two independent experimenters (R.L. and F.V.) blind to the diagnosis manually confirmed the EEG segments accepted for further analysis. Of note, special attention was devoted to avoid the inclusion of EEG segments and individual data sets with EEG signs of drowsiness or pre-sleep stages. Furthermore, the experimenters were blind to the diagnosis of the subjects at the moment of the preliminary EEG data analysis. Finally, we re-referenced artifact free EEG data to common average for further analysis.

Spectral analysis of the EEG data

A digital FFT-based power spectrum analysis (Welch technique, Hanning windowing function, no phase shift) computed power density of the EEG rhythms with 0.5 Hz frequency resolution. The following standard band frequencies were studied: delta (2–4 Hz), theta (4–8 Hz), alpha 1 (8–10.5 Hz), alpha 2 (10.5–13 Hz), beta 1 (13–20 Hz), and beta 2 (20–30 Hz). These band frequencies were chosen averaging those used in previous relevant EEG studies on dementia [29–32, 35, 52–71]. Sharing of a frequency bin by two contiguous bands is a widely accepted procedure [52, 54, 72–75]. Furthermore, this fits the theoretical consideration that near EEG rhythms may overlap at their frequency borders [29–32, 35, 57–71, 76–79].

Choice of the fixed EEG bands did not account for individual alpha frequency (IAF) peak, defined as the frequency associated with the strongest EEG power at the extended alpha range [77]. The mean IAF peak was 8.8 ± 0.2 Hz for the LC patients and 9.2 ± 0.2 Hz for the Nold subjects. Furthermore, the mean IAF peak was 7.9 ± 0.3 Hz for the CHE patients, 9.7 ± 0.3 Hz for the aMCI subjects, and 8.9 ± 0.4 Hz for the AD subjects. To control the effect of IAF on the EEG comparisons, the IAF peak was used as a covariate (together with age and gender) for further statistics.

Finally, the analysis of the delta band was restricted to 2–4 Hz for homogeneity with previously quoted field literature [29–32, 35, 57–71] and to avoid the residual effects of uncontrolled head movements, provoking artifactual power enhancement at low frequency delta band.

Cortical source analysis of the EEG rhythms by LORETA

Low resolution electromagnetic source tomography (LORETA) was used for the EEG source analysis as provided at http://www.unizh.ch/keyinst/NewLORETA/LORETA01.htm [80–82]. LORETA is a functional imaging technique belonging to a family of linear inverse solution procedures modeling 3D distributions of EEG sources [82]. With respect to the dipole modeling of cortical sources, LORETA estimation implies no *a priori* decision on the dipole position. Furthermore, LORETA is quite efficient when compared to other linear inverse algorithms like minimum norm solution, weighted minimum norm solution or weighted resolution optimization [81–84]. Finally, LORETA has been successfully used in recent

Table 3
Statistical ANOVA comparison distinguishing LC and Nold groups

	Central	Frontal	Parietal	Occipital	Temporal	Limbic
Theta	$p < 0.00003$		$p < 0.00003$	$p < 0.00003$	$p < 0.00003$	$p < 0.00003$
Alpha 1	$p < 0.001$	$p < 0.001$	$p < 0.001$		$p < 0.001$	$p < 0.001$
Alpha 2	$p < 0.002$		$p < 0.002$		$p < 0.002$	

EEG studies on pathological brain aging [29–33, 35, 57–71].

LORETA computes 3D linear solutions (LORETA solutions) for the EEG inverse problem within a 3-shell spherical head model including scalp, skull, and brain compartments. The brain compartment is restricted to the cortical gray matter/hippocampus of a head model co-registered to the Talairach probability brain atlas and digitized at the Brain Imaging Center of the Montreal Neurological Institute [85]. This compartment includes 2,394 voxels (7 mm resolution), each voxel containing an equivalent current dipole.

LORETA can be used from EEG data collected by low spatial sampling of 10–20 system (19 electrodes) when cortical sources are estimated from resting state EEG rhythms [29–32, 35, 57–71, 86–89]. LORETA solutions consisted of voxel z-current density values able to predict EEG spectral power density at scalp electrodes, being a reference-free method of EEG analysis, in that one obtains the same LORETA source distribution for EEG data referenced to any reference electrode including common average. A normalization of the data was obtained by normalizing the LORETA current density at each voxel with the power density averaged across all frequencies (0.5–45 Hz) and across all 2394 voxels of the brain volume. After the normalization, the solutions lost the original physical dimension and were represented by an arbitrary unit scale. The general procedure fitted the LORETA solutions in a Gaussian distribution and reduced intersubject variability [55].

Solutions of the EEG inverse problem are underdetermined and ill conditioned when the number of spatial samples (electrodes) is lower than that of the unknown samples (current density at each voxel). To account for that, the cortical LORETA solutions predicting scalp EEG spectral power density were regularized to estimate distributed rather than punctual EEG source patterns [80–82]. In line with the low spatial resolution of the adopted technique, homemade MATLAB software averaged the amplitude of LORETA solutions for all voxels belonging to each macroregion of interest such as frontal, central, parietal, occipital, temporal, and limbic. Each of these macroregions of interest (ROIs) was constituted by all the voxels of the Brodmann areas listed in Table 2. The belonging of a LORETA voxel to a Brodmann area was defined by original LORETA package.

Finally, the main advantage of the regional analysis of LORETA solutions—using an explicit source model coregistered into Talairach space—was that our modeling could disentangle rhythms of contiguous cortical areas (namely those from the occipital source were disentangled with respect to those of the contiguous parietal and temporal sources, etc.).

Statistical analyses

Results are expressed as mean ± standard error (SE), unless otherwise indicated. To test the working hypothesis, the following three statistical sessions were performed.

The first session tested the hypothesis that cortical (LORETA) sources of EEG rhythms differed in amplitude between LC and Nold subjects. To this aim, the regional normalized LORETA solutions from LC (including subjects with and without cognitive deficits) and Nold subjects were used as an input for an ANOVA design using age, gender, and IAF as covariates. Mauchley's test evaluated the sphericity assumption, and the correction of the degrees of freedom was made by Greenhouse–Geisser procedure. Duncan test was used for *post-hoc* test comparisons ($p < 0.05$). The ANOVA used the factors Group (Nold, LC; independent variable), Band (delta, theta, alpha 1, alpha 2, beta 1, beta 2), and ROI (central, frontal, parietal, occipital, temporal, limbic). The working hypothesis would be confirmed by the following two statistical results: (i) a statistical ANOVA effect including the factor Group ($p < 0.05$); (ii) a *post-hoc* test indicating statistically significant differences of the regional normalized LORETA solutions with the patterns LC $\neq$ Nold (Duncan test, $p < 0.05$).

The second session tested the hypothesis that in LC patients, the activity of cortical (LORETA) sources of EEG rhythms was related to psychometric measures. To this aim, we performed a correlation analysis (Pearson test, $p < 0.01$) between the amplitude of regional normalized LORETA solutions and mean Z psychometric score (MZPS) in LC patients. To reduce the amount

of univariate comparisons, only the regional normalized LORETA solutions fitting the pattern LC $\neq$ Nold were considered for that correlation analysis.

The third session tested the hypothesis that cortical (LORETA) sources of EEG rhythms differed in amplitude activity in CHE patients with respect to Nold, aMCI, and AD subjects. To this aim, the regional normalized LORETA solutions from the CHE, Nold, aMCI, and AD subjects were used as an input for an ANOVA design using age, gender, and IAF as covariates. The ANOVA used the factors Group (Nold, aMCI, AD, CHE; independent variable), Band (delta, theta, alpha 1, alpha 2, beta 1, beta 2), and ROI (central, frontal, parietal, occipital, temporal, limbic). The working hypothesis would be confirmed by the following two statistical results: (i) a statistical ANOVA effect including the factor Group ($p < 0.05$); (ii) a *post-hoc* test indicating statistically significant differences of the regional normalized LORETA solutions with the patterns CHE $\neq$ Nold, aMCI, AD (Duncan test, $p < 0.05$).

RESULTS

Topography of the EEG cortical sources estimated in the LC and Nold groups

For illustrative purposes, Fig. 1 maps the grand average of the LORETA solutions (i.e., relative current density at cortical voxels) modeling cortical sources of delta, theta, alpha 1, alpha 2, beta 1, and beta 2 rhythms in the Nold and LC groups. The Nold group presented alpha 1 sources with the maximal values of power distributed in parietal and occipital regions. Delta, theta, and alpha 2 sources had moderate activity amplitude values when compared to alpha 1 sources. Furthermore, beta 1 and beta 2 sources were characterized by lowest activity. Compared to the Nold group, the LC group showed an activity increase of widespread theta, alpha 1, and alpha 2 sources.

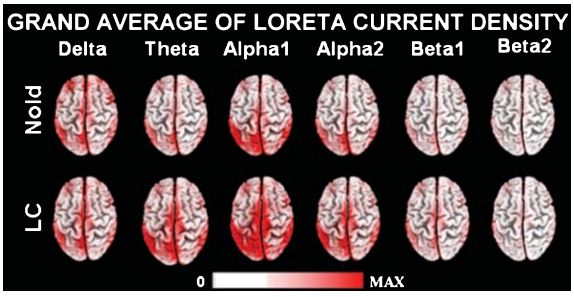

Fig. 1. Grand average of the LORETA solutions (i.e., normalized relative current density at the cortical voxels) modeling cortical sources of delta, theta, alpha 1, alpha 2, beta 1, and beta 2 rhythms in the Nold and LC subjects. The left side of the maps (top view) corresponds to the left hemisphere. LORETA, low-resolution brain electromagnetic tomography.

Statistical comparisons of the EEG cortical sources estimated in the LC and Nold groups

The ANOVA for the evaluation of the first working hypothesis (i.e., amplitude difference of cortical LORETA sources of EEG rhythms between the LC and Nold groups) showed a statistically significant interaction ($F(25,3150) = 4.48$; $p < 0.0001$) among the factors Group (Nold, LC), Band (delta, theta, alpha 1, alpha 2, beta 1, and beta 2), and ROI (central, frontal, parietal, occipital, temporal, limbic). Figure 2 shows the mean regional normalized LORETA solutions relative to this statistical ANOVA interaction. In the figure, the regional normalized LORETA solutions had the shape of EEG relative power spectra. Notably, profile and magnitude of these spectra in the Nold and LC groups differed across diverse cortical macro-regions, thus supporting the idea that scalp EEG rhythms are generated by a distributed pattern of cortical sources. The Duncan planned *post-hoc* testing (Table 3) showed that the source pattern LC $\neq$ Nold was fitted by theta (central, parietal, occipital, temporal, and limbic areas; $p < 0.00003$), alpha 1 (central, frontal, parietal, temporal, and limbic areas; $p < 0.001$), and alpha 2 (central, parietal, and temporal areas; $p < 0.002$) sources, where the amplitude of LORETA sources was stronger in the LC compared to the Nold subjects.

To explore the relationship between the cortical EEG rhythms and subjects' global cognitive functions, the normalized regional LORETA sources were used as an input for the correlation with the MZPS in all LC subjects (Pearson test, $p < 0.01$). The MZPS showed a statistically significant negative correlation with central ($r = -0.32$, $p = 0.008$), parietal ($r = -0.45$, $p = 0.0002$), and temporal ($r = -0.45$, $p = 0.0002$) theta sources. Furthermore, the MZPS showed a statistically significant positive correlation with parietal ($r = 0.34$, $p = 0.005$) and temporal alpha 2 ($r = 0.33$, $p = 0.009$) sources. Figure 3 shows the scatterplots of these statistically significant correlations.

Topography of the EEG cortical sources estimated in the CHE compared to the control groups

For illustrative purposes, Fig. 4 maps the grand average of the LORETA solutions (i.e., relative current

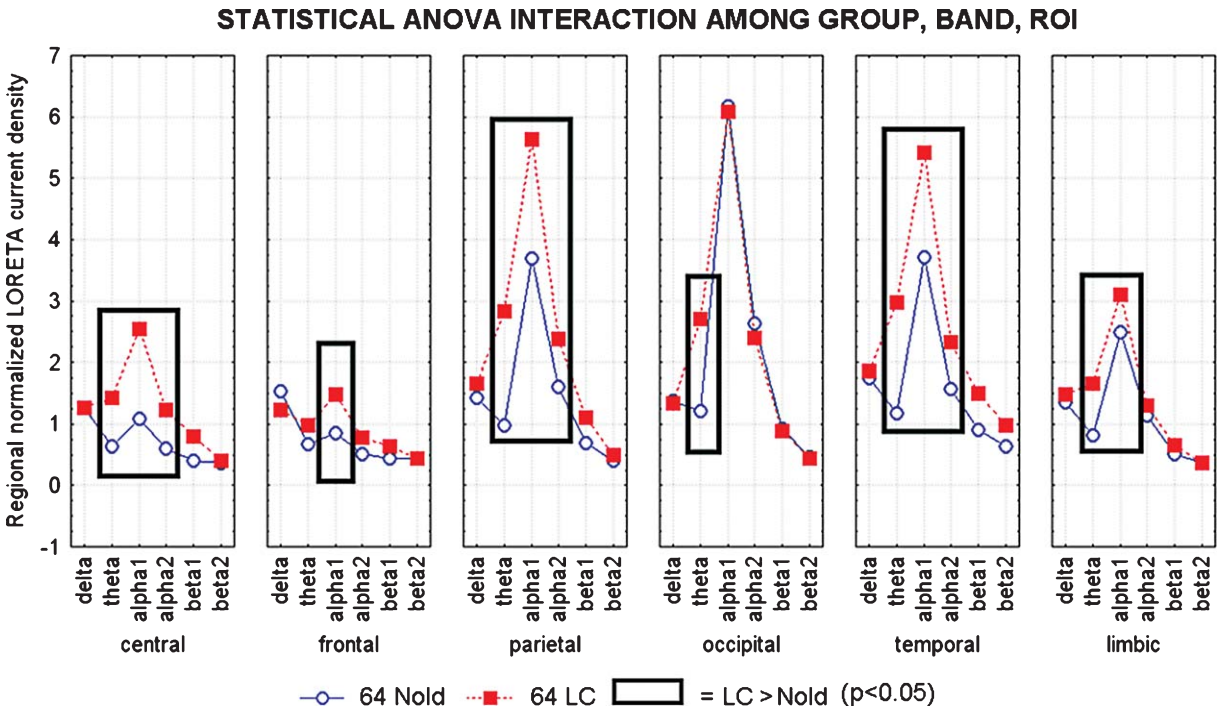

Fig. 2. Regional normalized LORETA solutions (mean across subjects) relative to a statistical ANOVA interaction among the factors Group (Nold, LC), Band (delta, theta, alpha 1, alpha 2, beta 1, and beta 2), and Region of interest (central, frontal, parietal, occipital, temporal, limbic). This ANOVA design used the regional normalized LORETA solutions as a dependent variable. Subjects' age, gender and individual alpha frequency peak were used as covariates. Regional normalized LORETA solutions modeled the EEG relative power spectra as revealed by a sort of "virtual" intracranial macro-electrodes located on the macrocortical regions of interest. The rectangles indicate the cortical regions and frequency bands in which LORETA solutions presented statistically significant LORETA patterns LC $\neq$ Nold ($p < 0.05$). Nold, normal elderly subjects; LC, liver cirrhosis; LORETA, low resolution brain electromagnetic source topography.

density at cortical voxels) modeling cortical sources of delta, theta, alpha 1, alpha 2, beta 1, and beta 2 rhythms in the Nold, aMCI, AD, and CHE groups. Compared to the Nold group, the AD group showed an increase of widespread delta sources, along with a dramatic reduction of parieto-occipital alpha 1 sources. With respect to the Nold and AD groups, the aMCI group showed intermediate magnitude of alpha 1 sources. Finally, the CHE group was characterized by an amplitude increase of widespread theta and centro-parietal alpha 1 sources compared to the Nold, MCI and AD groups.

Statistical comparisons of the EEG cortical sources estimated in the CHE compared to the control groups

An ANOVA compared the cortical sources of EEG rhythms in the Nold (specifically the sub-group of Nold subjects matched to pathological groups), aMCI, AD, and CHE groups. Results showed a statistically significant interaction ($F(75,2) = 4.68$; $p < 0.0001$) among the factors Group (Nold, aMCI, AD, CHE), Band (delta, theta, alpha 1, alpha 2, beta 1, and beta 2), and ROI (central, frontal, parietal, occipital, temporal, limbic). Figure 5 shows the mean regional normalized LORETA solutions relative to this statistical ANOVA interaction. The Duncan planned *post-hoc* testing showed that the source pattern of interest CHE $\neq$ Nold, aMCI, and AD was fitted by theta (central, parietal, occipital, temporal, and limbic areas; $p < 0.002$) and alpha 1 (central, frontal, parietal, temporal, and limbic; $p < 0.02$) sources, where the amplitude of LORETA sources was stronger in the CHE group than in the Nold, aMCI, and AD groups. Noteworthy, the power of the theta sources did not differ among the Nold, aMCI, and AD groups ($p > 0.05$).

Control analysis of EEG functional coupling

As previously mentioned, theta (central, parietal, occipital, temporal, and limbic areas), alpha 1 (central, frontal, parietal, temporal, and limbic areas), and alpha 2 (central, parietal, and temporal areas) LORETA sources were higher in power in the LC then Nold

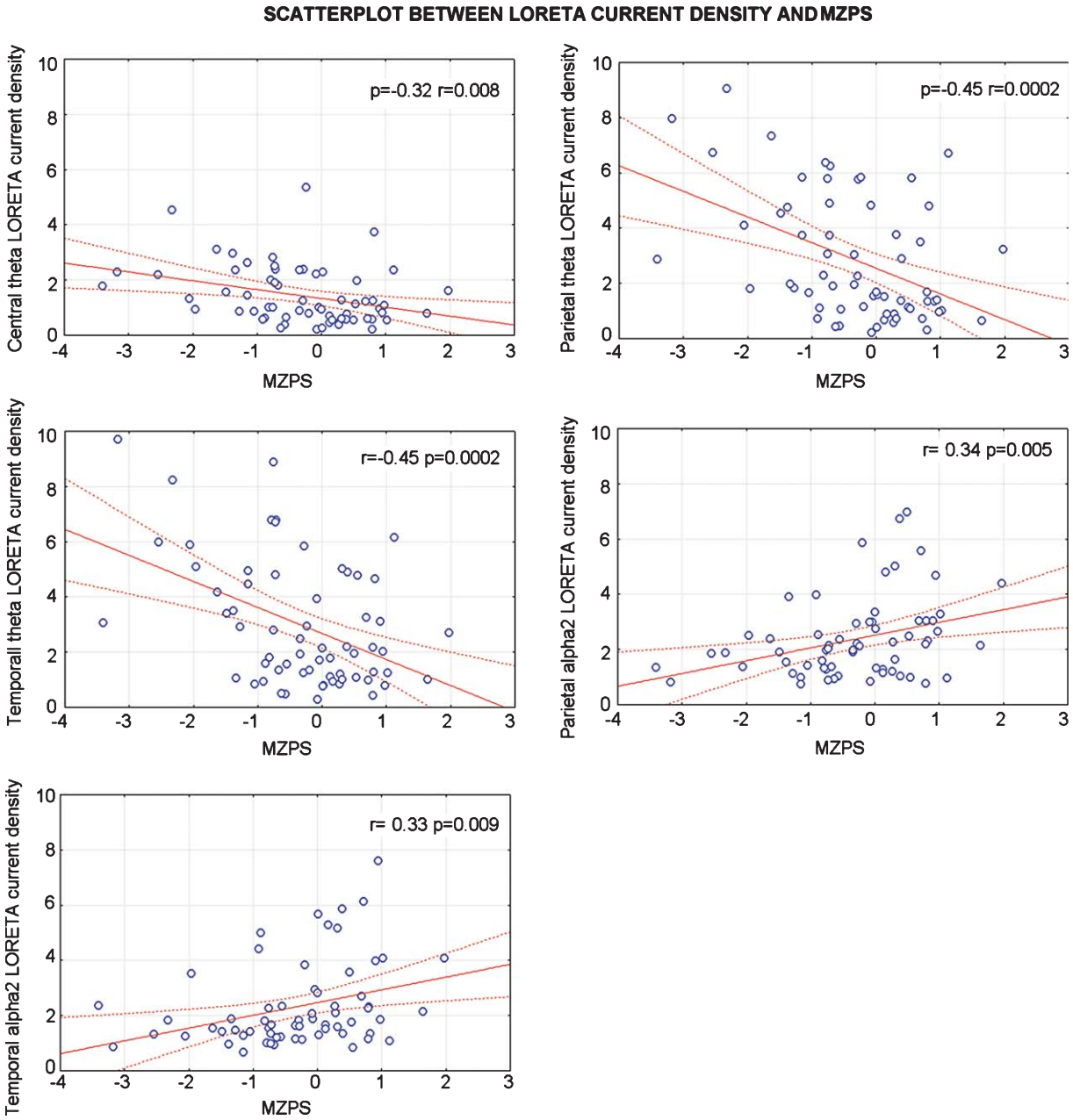

Fig. 3. Scatterplots showing the correlation between regional normalized LORETA solutions and mean Z psychometric score (MZPS) in the LC subjects. The *r*- and *p*-values refer to Pearson correlation are reported within the diagram.

groups. These results raised the issue about the functional meaning of increased alpha rhythms in the LC patients in the light of the well-known assumption that healthy cortical neural synchronization is reflected by low-amplitude theta rhythms and high-amplitude alpha rhythms in the resting state eyes-closed condition. A control analysis was performed to evaluate whether the high amplitude of alpha sources in the LC patients was associated to an abnormal functional coupling of resting state EEG rhythms, as a sign of an abnormal "networking" between paired cortical regions. To address this issue, we evaluated the EEG spectral coherence in the LC and Nold subjects. Indeed, EEG spectral coherence between electrode pairs is commonly interpreted as an index of functional coupling [90, 91], mutual information exchange [92], functional

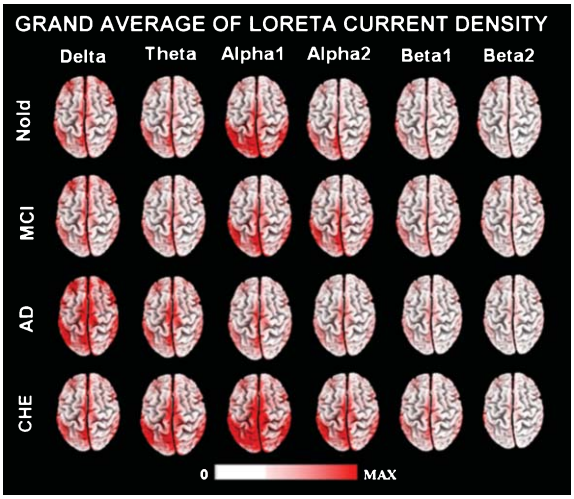

Fig. 4. Grand average of the LORETA solutions (i.e., normalized relative current density at the cortical voxels) modeling cortical sources of delta, theta, alpha 1, alpha 2, beta 1, and beta 2 rhythms in the normal elderly subjects (Nold), mild cognitive impairment (MCI), Alzheimer's disease (AD), and covert hepatopatic hencephalopathy (CHE) subjects. The left side of the maps (top view) corresponds to the left hemisphere.

co-ordination [93], and integrity of cortical neural pathways [94]. Its basic theoretical assumption is that when the activity of two cortical areas is functionally coordinated, the EEG rhythms of these cortical areas show linear interrelatedness and high spectral coherence. Shortly, EEG coherence is a normalized measure of the coupling between two signals at any given frequency [92, 95]. From a physiological point of view, EEG coherence reflects functional cooperation among the brain areas under study. In the present study, the coherence values were calculated for each frequency bin by (Eq. 1)

$$Coh_{xy}(\lambda) = \left|R_{xy}(\lambda)\right|^2 = \frac{\left|f_{xy}(\lambda)\right|^2}{f_{xx}(\lambda) f_{yy}(\lambda)}. \quad (1)$$

The above equation is the extension of the Pearson's correlation coefficient to complex number pairs. In this equation, f denotes the spectral estimate of two EEG signals x and y for a given frequency bin (λ). The numerator contains the cross spectrum for x and y (f_{xy}), while the denominator contains the respective autospectra for x (f_{xx}) and y (f_{yy}). For each frequency bin (λ), the coherence value (Coh_{xy}) is obtained by squaring the magnitude of the complex correlation coefficient R. This procedure returns a real number between 0 (no coherence) and 1 (maximal coherence).

In line with previous studies of the present research group [61, 96–102], the spectral coherence between couples of electrodes was calculated by a home-made software developed under Matlab 6.5 (Mathworks Inc., Natrick, MA; an extension of Pearson's correlation coefficient to complex number pairs; 1-Hz frequency resolution). Specifically, the calculation of the coherence was performed from the artifact-free EEG data, on the basis of all scalp electrodes used during EEG recordings. The coherence was computed at theta (4–8 Hz), alpha 1 (8–10.5 Hz), and alpha 2 (10.5–13 Hz) bands.

For the evaluation of the frontal intra-hemispheric functional coupling, the EEG spectral coherence was evaluated between frontal and other cortical regions. In particular, the EEG spectral coherence was evaluated between the following electrode pairs of interest: F3-C3, F3-P3, F3-T3, F3-O1, F4-C4, F4-P4, F4-T4, and F4-O2. For the evaluation of the central intra-hemispheric functional coupling, the EEG spectral coherence was evaluated between central and other cortical regions (i.e., C3-F3, C3-P3, C3-T3, C3-O1, C4-F4, C4-P4, C4-T4, and C4-O2). For the evaluation of the parietal intra-hemispheric functional coupling, the EEG spectral coherence was evaluated between parietal and other cortical regions (i.e., P3-F3, P3-C3, P3-T3, P3-O1, P4-F4, P4-C4, P4-T4, and P4-O2). For the evaluation of the temporal intra-hemispheric functional coupling, the EEG spectral coherence was evaluated between temporal and other cortical regions (i.e., T3-F3, T3-C3, T3-P3, T3-O1, T4-F4, T4-C4, T4-P4, and T4-O2). For the evaluation of the occipital intra-hemispheric functional coupling, the EEG spectral coherence was evaluated between occipital and other cortical regions (i.e., O1-F3, O1-C3, O1-P3, O1-T3, O2-F4, O2-C4, O2-P4, and O2-T4).

In total, we performed five ANOVAs having the coherence as a dependent variable and age, gender, and IAF as covariates. For the evaluation of frontal intra-hemispheric functional coupling, the ANOVA factors were Group (Nold, LC), Band (theta, alpha 1, alpha 2), Region of interest (frontal-central, frontal-parietal, frontal-temporal, frontal-occipital), and Hemisphere (left, right). Electrode pairs of interest were F3-C3 and F4-C4 (frontal-central), F3-P3 and F4-P4 (frontal-parietal), P3-T3 and P4-T4 (frontal-temporal), and P3-O1 and P4-O2 (frontal-occipital). The ANOVA showed a statistically significant interaction ($F(6,756) = 2.2$; $p < 0.05$) among the factors Group, Band, and ROI (see Fig. 6A). Duncan *post-hoc* testing indicated that the bilateral frontal-central and frontal-occipital theta coherence was higher in the LC than Nold subjects ($p < 0.01$). On the contrary, bilateral frontal-parietal and frontal-temporal alpha 1 and alpha

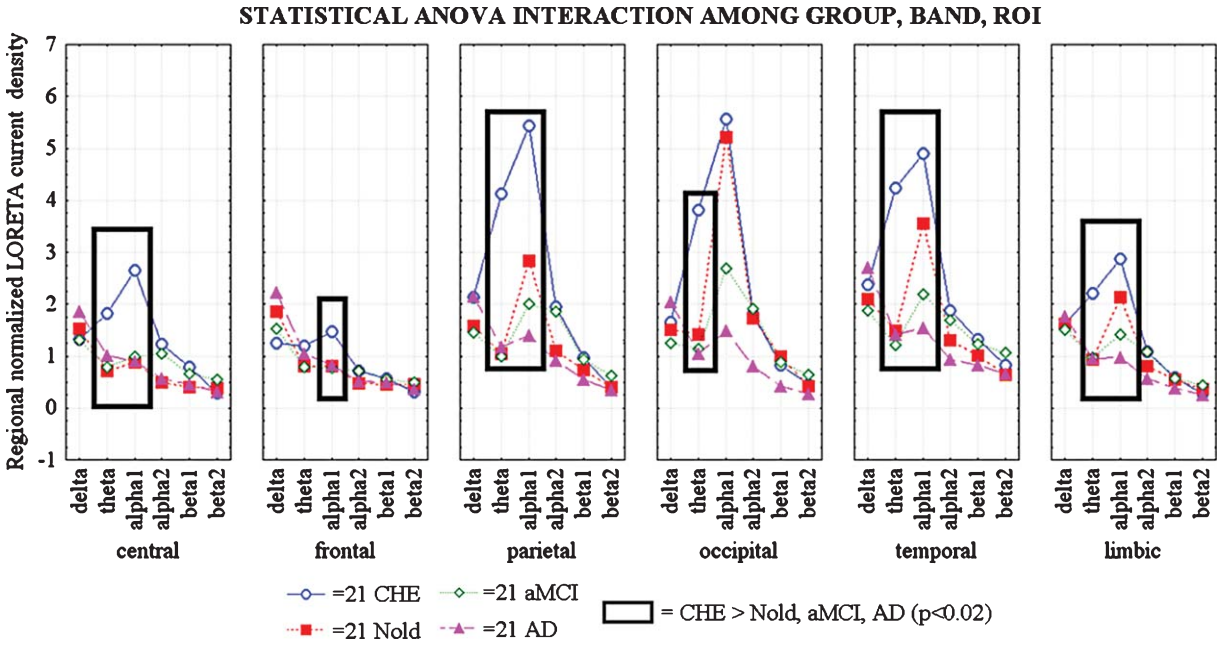

Fig. 5. Regional normalized LORETA solutions (mean across subjects) relative to a statistical ANOVA interaction among the factors Group (Nold, MCI, AD, CHE), Band (delta, theta, alpha 1, alpha 2, beta 1, and beta 2), and Region of interest (central, frontal, parietal, occipital, temporal, limbic). This ANOVA design used the regional normalized LORETA solutions as a dependent variable. Subjects' age, gender and individual alpha frequency peak were used as covariates. The rectangles indicate the cortical regions and frequency bands in which LORETA solutions presented statistically significant LORETA patterns CHE $\neq$ Nold, MCI, AD ($p < 0.05$).

2 coherence was lower in the LC than Nold subjects ($p < 0.01$).

For the evaluation of central intra-hemispheric functional coupling, the ANOVA factors were Condition (Nold, LC), Band (theta, alpha 1, alpha 2), Region of interest (central-frontal, central-parietal, central-temporal, central-occipital), and Hemisphere (left, right). Electrode pairs of interest were C3-F3 and C4-F4 (central-frontal), C3-P3 and C4-P4 (central-parietal), C3-T3 and C4-T4 (central-temporal), and C3-O1 and C4-O2 (central-occipital). The ANOVA showed a statistically significant interaction ($F(6,756) = 3.32$; $p < 0.003$) among the factors Group, Band, and ROI (see Fig. 6B). Duncan *post-hoc* testing indicated that the bilateral central-frontal and central-occipital theta coherence was higher in the LC than Nold subjects ($p < 0.01$). On the contrary, bilateral central-temporal alpha 2 coherence was lower in the HE than in Nold subjects ($p < 0.02$).

For the evaluation of parietal intra-hemispheric functional coupling, the ANOVA factors were Group (Nold, LC), Band (theta, alpha 1, alpha 2), Region of interest (parietal-frontal, parietal-central, parietal-temporal, parietal-occipital), and Hemisphere (left, right). Electrode pairs of interest were P3-F3 and P4-F4 (parietal-frontal), P3-C3 and P4-C4 (parietal-central), P3-T3 and P4-T4 (parietal-temporal), and P3-O1 and P4-O2 (parietal-occipital). The ANOVA showed a statistically significant interaction ($F(6,756) = 3.94$; $p < 0.0007$) among the factors Group, Band, and ROI (see Fig. 6C). Duncan *post-hoc* testing indicated that the bilateral parietal-occipital theta coherence as well as bilateral parietal-frontal and parietal-occipital alpha 1 and alpha 2 coherence was lower in the LC than Nold subjects ($p < 0.04$).

For the evaluation of temporal intra-hemispheric functional coupling, the ANOVA factors were Condition (Nold, LC), Band (theta, alpha 1, alpha 2), Region of interest (temporal-frontal, temporal-central, temporal-parietal, temporal-occipital), and Hemisphere (left, right). Electrode pairs of interest were T3-F3 and T4-F4 (temporal-frontal), T3-C3 and T4-C4 (temporal-central), T3-P3 and T4-P4 (temporal-parietal), and P3-O1 and T4-O2 (temporal-occipital). The ANOVA showed a statistically significant interaction ($F(6,756) = 6.54$; $p < 0.0001$) among the factors Group, Band, and ROI (see Fig. 6D). Duncan *post-hoc* testing indicated that the bilateral temporal-frontal, temporal-parietal, and temporal-occipital alpha 1 coherence was lower in the LC than Nold subjects ($p < 0.01$). Similarly, the bilateral temporal-frontal, temporal-central, and temporal-occipital alpha 2

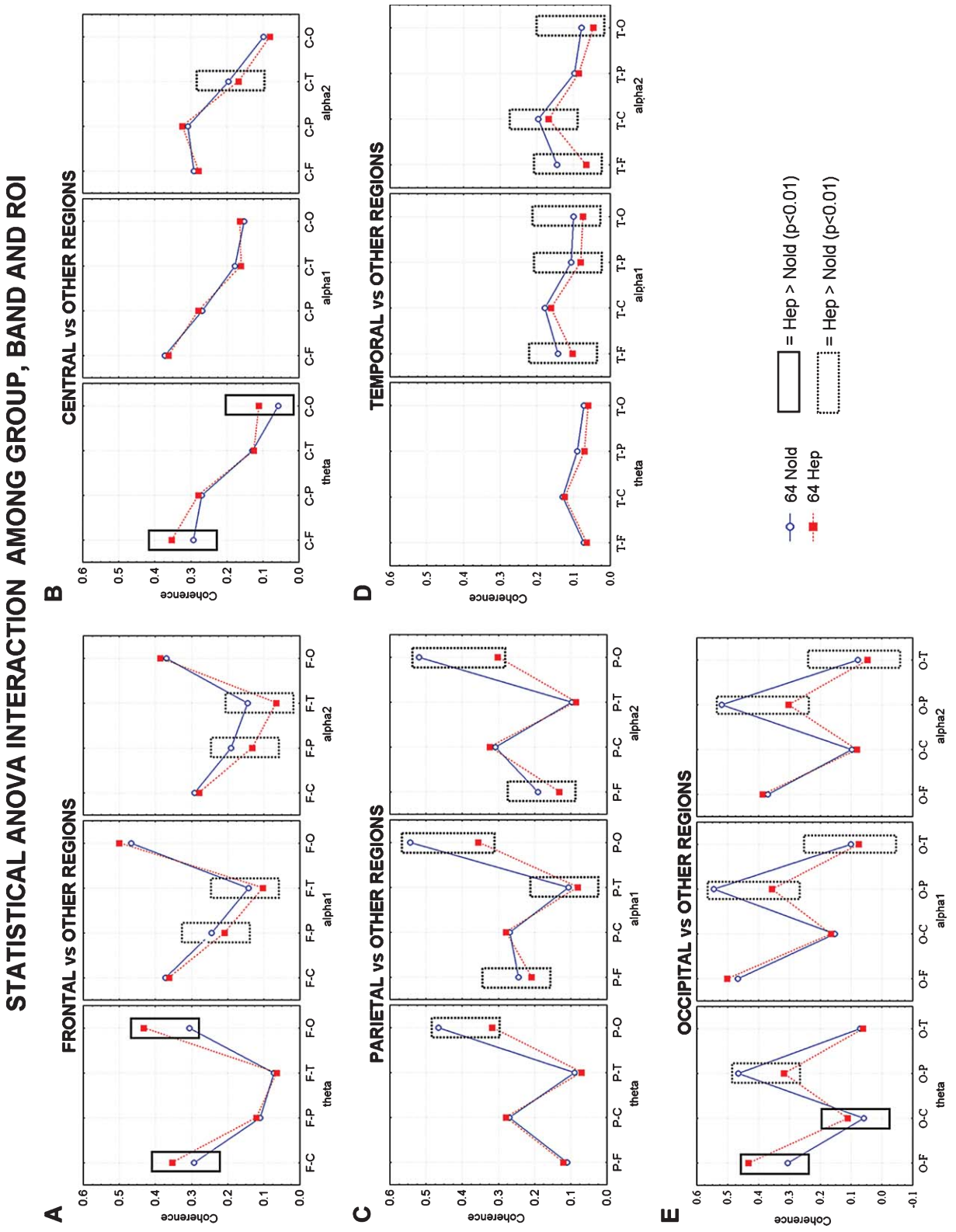
STATISTICAL ANOVA INTERACTION AMONG GROUP, BAND AND ROI
A
FRONTAL vs OTHER REGIONS
B
CENTRAL vs OTHER REGIONS
C
PARIETAL vs OTHER REGIONS
D
TEMPORAL vs OTHER REGIONS
E
OCCIPITAL vs OTHER REGIONS
Coherence
theta
alpha1
alpha2
64 Nold
64 Hep
= Hep > Nold (p<0.01)
= Hep > Nold (p<0.01)

coherence was lower in LC compared to Nold subjects ($p < 0.01$).

For the evaluation of occipital intra-hemispheric functional coupling, the ANOVA factors were Group (Nold, LC), Band (theta, alpha 1, alpha 2), Region of interest (occipital-frontal, occipital-central, occipital-temporal, occipital-parietal), and Hemisphere (left, right). Electrode pairs of interest were O1-F3 and O2-F4 (occipital-frontal), O1-C3 and O2-C4 (occipital-central), O1-T3 and O1-T4 (occipital-temporal), and O1-P3 and O2-P4 (occipital-parietal). The ANOVA showed a statistically significant interaction ($F(6,756) = 4.67$; $p < 0.0007$) among the factors Group, Band, and ROI (see Fig. 6E). Duncan *post-hoc* testing indicated that the bilateral occipital-frontal and occipital-central theta coherence was higher in LC compared to Nold subjects ($p < 0.001$). On the contrary, the bilateral occipital-parietal, occipital-temporal alpha 1 and alpha 2 coherence as well as occipital-parietal theta coherence were lower in the LC than Nold subjects ($p < 0.01$).

On the whole, the results of this control analysis suggest that compared to the Nold subjects, the LC patients were characterized by higher functional coupling of the pathological theta rhythms and lower functional coupling of the dominant alpha rhythms. These control results suggest that in the LC patients, the abnormally high activity of alpha sources is associated with an abnormal functional coupling of the resting state EEG rhythms.

DISCUSSION

In the present study, we tested the hypothesis that compared to control subjects, LC patients are characterized by widespread abnormalities of the cortical sources of resting state EEG rhythms as spatial distribution and frequency bands, as an effect of the generalized action of circulating neurotoxins (e.g., ammonia) on the whole brain. As a methodological novelty, we used a validated approach for the estimation of the cortical sources of resting state EEG rhythms that allowed a useful spatial analysis of the abnormal brain synchronization mechanisms generating these rhythms in elderly subjects with cognitive decline [29–32, 35].

Results showed that widely distributed sources of theta (all but frontal), alpha 1 (all but occipital), and alpha 2 (parietal, temporal) rhythms were higher in amplitude in all LC patients than in the Nold subjects. Furthermore, the amplitude of central, parietal, and temporal theta sources correlated negatively, and parietal and temporal alpha 2 sources correlated positively with an index of global cognitive status across all LC patients. These results confirm and extend to the fine detail of the cortical source level previous evidence showing that EEG theta and alpha band power computed at scalp electrodes was related to psychometric performance in LC patients, and differed in amplitude between LC patients and matched healthy controls [18, 19, 22]. Furthermore, these effects are fully in line with the so called "anteriorization" of theta and alpha rhythms previously described in HE patients by independent groups, which were ascribed to some processes of drowsiness preceding sleep onset [23–27]. However, it is improbable that occasional sleep onset during the EEG recordings can explain the present results, as this aspect was carefully monitored by the experimenters and alpha rhythms typically drop down at the sleep onset. Therefore, a possible slight reduction of the vigilance might have other reasons related to HE pathophysiology *per se*.

As a novelty of the present study, we tested the hypothesis of peculiar abnormalities in the spatial distribution and frequency bands of the cortical sources of resting state EEG rhythms in patients with CHE when compared to patients with possible prodromal (i.e., aMCI) or overt AD. The CHE patients were expected to show widespread abnormalities of the cortical sources of EEG rhythms due to the diffuse action of the pathological agents affecting brain activity and cognitive processes. In contrast, the MCI and AD patients were expected to be characterized by

Fig. 6. A) Intra-hemispheric frontal coherence (mean across subjects) relative to a statistical ANOVA interaction among the factors Group (Nold, LC), Band (theta, alpha 1, alpha 2), and ROI (frontal-central, frontal-parietal, frontal-temporal, frontal-occipital). B) Intra-hemispheric central coherence (mean across subjects) relative to a statistical ANOVA interaction among the factors Group (Nold, LC), Band (theta, alpha 1, alpha 2), and Region of interest (central-frontal, central-parietal, central-temporal, central-occipital). C) Intra-hemispheric parietal coherence (mean across subjects) relative to a statistical ANOVA interaction among the factors Group (Nold, LC), Band (theta, alpha 1, alpha 2), and Region of interest (parietal-frontal, parietal-central, parietal-temporal, parietal-occipital). D) Intra-hemispheric temporal coherence (mean across subjects) relative to a statistical ANOVA interaction among the factors Group (Nold, LC), Band (theta, alpha 1, alpha 2), and Region of interest (temporal-frontal, temporal-central, temporal-parietal, temporal-occipital). E) Intra-hemispheric temporal coherence (mean across subjects) relative to a statistical ANOVA interaction among the factors Group (Nold, LC), Band (theta, alpha 1, alpha 2), and Region of interest (occipital-frontal, occipital-central, occipital-temporal, occipital-parietal). Rectangles indicate the electrode pairs at which coherence presented the statistically significant pattern LC $\neq$ Nold ($p < 0.05$).

more circumscribed spatial and frequency abnormalities of these EEG rhythms as the main target of the neurodegenerative processes is typically localized in hippocampus and posterior cortical regions. The confirmation of the working hypothesis would confirm that the present methodological approach can shed light on the understanding of the peculiar abnormalities in the generation of the resting state EEG rhythms in people with cognitive decline due to different patho-physiological mechanisms such as CHE and MCI/AD. It should be remarked that at this early stage of the research, we followed the standard clinical guidelines for the clinical diagnosis of CHE, which is based on the pooling of patients with both MHE (i.e., diagnosed based on objective cognitive deficits as revealed by psychometric tests) and West Haven grade I HE (i.e., diagnosed based on a structured clinical evaluation, which is less reproducible than psychometric testing). This approach was implemented in the framework of our daily clinical routine. In light of the present encouraging findings, future confirmatory studies should systematically carry out psychometric testing in the enrolled LC patients to select only those having statistically significant sub-clinical cognitive deficits.

Results showed a different spatial-frequency pattern of the EEG sources between CHE and aMCI or AD patients, thus disclosing the diverse early effects of the HE and AD processes on the resting state cortical EEG rhythms. Specifically, widely distributed theta (all but frontal) and alpha 1 (all but occipital) sources showed higher activity in the sub-group of LC patients with CHE than in the patients with aMCI or AD. A plausible explanation of the results is that enhanced theta sources in the LC patients may be interpreted according to the general view that the high amplitude of the low-frequency EEG rhythms (about 1–7 Hz) reflects the abnormal interactions between thalamic and cortical neural populations, resulting in a functional isolation of cortical modules [56, 77, 103–108]. The main known causes of this condition are cortical hypoperfusion, neurotrauma, or neurodegeneration [29, 56, 107–109]. In this theoretical line, the present results lend support to the notion that hepatic metabolic disorders may widely influence these mechanisms as well. With respect to the progressive AD neurodegenerative processes mainly affecting hippocampus and posterior cortical regions at early disease stages, the LC processes might exert acute and widely spread effects on the brain, thus inducing stronger pathological effects on the thalamo-cortical mechanisms generating the resting state theta rhythms.

Another interesting result of the present study is that the cortical sources of alpha rhythms were higher in power in the CHE patients than in the control subjects (i.e., Nold, aMCI, and AD). These results may be interpreted at the light of the general theory on the generation of the resting state alpha rhythms in humans. Low frequency (about 8–10.5 Hz) alpha rhythms would denote the synchronization of diffuse neural networks regulating the fluctuation of subject's global arousal and consciousness states, whereas high frequency (about 10.5–13 Hz) alpha rhythms would denote the synchronization of more selective neural networks specialized in the processing of modal specific or semantic information [76, 78, 79]. Keeping in mind the above theoretical considerations, a plausible explanation of the results is that AD neurodegeneration and CHE differently impinge upon the neural mechanism at the basis of the generation of resting state alpha rhythms, which is one of main mechanisms regulating the cortical arousal and vigilance. Therefore, the present results suggest that cognitive deficits of the MCI/AD and CHE patients may be related to a diverse alteration of the cortical arousal. The MCI/AD subjects were characterized by a tonic de-synchronization of the resting state alpha rhythms as a reflection of a tonic cortical excitation. In contrast, the CHE patients were characterized by a tonic hyper-synchronization of the resting state alpha rhythms as a reflection of a tonic cortical inhibition. Both up- and down-regulation of cortical arousal would be associated with an abnormal brain function and predict cognitive deficits. Effective cognitive processing is expected to stem upon the selectivity and flexibility of the excitation and inhibition across brain neural networks during both resting state condition and task demands (see, for example, the concept of "neural efficiency"; [110–113]). The plausibility of the above explanation is related to the well-known relationship between the fluctuation of the cortical arousal in the condition of the resting state and the power of the cortical alpha rhythms [76, 78, 79].

Less clear are the neurophysiological and neurobiological fine mechanisms linking the AD neurodegeneration, CHE neurotoxins, and the neurophysiological mechanisms generating the resting state cortical alpha rhythms. At this early stage of the research, we can just speculate that AD neurodegeneration and CHE neurotoxins exert their effects on the ascending neuro-modulatory systems at the basis of the resting state EEG rhythms and cortical arousal. However, the heuristic value of the present results should not be underestimated. They motivate future studies investigating the correlation among the present

neurophysiological (EEG) markers, the cognitive deficits, and direct indexes of up- and down-regulation of the mentioned ascending neuromodulatory systems. These future investigations should enlighten these interactions, unveiling the relationships between the alpha source pattern during the resting state condition and relevant indexes of the cholinergic, glutamatergic, and GABA modulation (note that GABA is the principal inhibitory neurotransmitter in the human brain and modulates cholinergic and glutamatergic activity in the neocortex and the hippocampus) [114]. These future investigations should test the hypothesis that the increase of the low-frequency alpha sources (i.e., tonic cortical inhibition) in the LC/HCE patients is related to an enhancement of the inhibitory GABA-ergic tone provoked by neurosteroids [115–117] and/or to a depression of the glutamate-nitric oxide-cGMP excitatory pathway [118]. Furthermore, the decrease of the low-frequency alpha sources (i.e., tonic cortical excitation) in the MCI or AD patients might be related to a reduction of the inhibitory GABA-ergic tone [114], to a depression of the cholinergic inhibitory activity, and/or to an enhancement of the excitatory glutamatergic non-NMDA receptor activity [119, 120]. Finally, it should be tested the role of the dopaminergic and serotoninergic systems on the modulation of the cortical sources of the resting state alpha rhythms in these patients [121, 122].

In conclusion, the present study tested the hypothesis that LC and AD conditions are characterized by peculiar abnormalities of the cortical sources of resting state EEG rhythms, reflecting the relative patho-physiological mechanisms. Compared to the control healthy subjects, the LC/CHE patients were characterized by widespread abnormalities of the cortical sources of the resting state theta and alpha rhythms. Furthermore, the cortical sources of the resting state alpha rhythms appeared to change differently under the influence of the LC/CHE and AD conditions. The patients with LC/CHE were characterized by widespread abnormalities as spatial distribution and frequency bands of the cortical sources of the theta, low- and high-frequency alpha rhythms. These findings are compatible with the widespread effects on brain activity provoked by the circulating byproducts of liver failure passing the brain-blood barrier. On the other hand, the patients with aMCI and AD showed a spatially selective derangement of the posterior cortical sources of the delta and low-frequency alpha rhythms, as expected by the typical specific track of the neurodegenerative processes in the earlier disease stages. These EEG markers are interesting candidates to capture the neurophysiological mechanisms of action of pharmacological interventions for the two pathologies, with promising perspectives for the development of new drugs, a better understanding of their neurophysiological mechanisms, and therapy monitoring. Finally, the findings of this exploratory study encourages further investigations on the cortical sources of the resting state EEG rhythms in the LC/CHE patients and in the aMCI/AD patients as a function of the effects of the therapy, disease progression, and activity of the main ascending neuromodulatory systems.

ACKNOWLEDGMENTS

This research was developed thank to the financial support by European Committee for the FP7-"ICT Infrastructure" project entitled "Diagnostic Enhancement of Confidence by an International Distributed Environment" ("DECIDE", Grant Agreement: RI-261593) in the framework of the validation of spectral electroencephalographic indexes in the differential diagnosis of Alzheimer's disease. Therefore, this article is presented on behalf of the DECIDE Consortium. Please find complete information about the Consortium and principal investigators at http://www.eu-decide.eu.

Authors' disclosures available online (http://www.j-alz.com/disclosures/view.php?id=1595).

REFERENCES

[1] Ferenci P, Lockwood A, Mullen K, Tarter R, Weissenborn K, Blei AT (2002) Hepatic encephalopathy–definition, nomenclature, diagnosis, and quantification: Final report of the working party at the 11th World Congresses of Gastroenterology, Vienna, 1998. *Hepatology* **35**, 716-721.

[2] Amodio P, Montagnese S, Gatta A, Morgan MY (2004) Characteristics of minimal hepatic encephalopathy. *Metab Brain Dis* **19**, 253-267.

[3] Ferenci P, Stauber R, Steindl-Munda P, Gschwantler M, Fickert P, Datz C, Müller C, Hackl F, Rainer W, Watkins-Riedel T, Lin W, Krejs GJ, Gangl A; Austrian Hepatitis Study Group (2001) Treatment of patients with chronic hepatitis C not responding to interferon with high-dose interferon alpha with or without ribavirin: Final results of a prospective randomized trial. Austrian Hepatitis Study Group. *Eur J Gastroenterol Hepatol* **13**, 699-705.

[4] Conn HO, Leevy CM, Vlahcevic ZR, Rodgers JB, Maddrey WC, Seeff L, Levy LL (1977) Comparison of lactulose and neomycin in the treatment of chronic portal-systemic encephalopathy. A double blind controlled trial. *Gastroenterology* **72**, 573-583.

[5] Bajaj JS, Cordoba J, Mullen KD, Amodio P, Shawcross DL, Butterworth RF, Morgan MY (2011) Review article: The design of clinical trials in hepatic encephalopathy–an International Society for Hepatic Encephalopathy and Nitrogen

Metabolism (ISHEN) consensus statement. *Aliment Pharmacol Ther* **33**, 739-747.

[6] Ortiz M, Jacas C, Cordoba J (2005) Minimal hepatic encephalopathy: Diagnosis, clinical significance and recommendations. *J Hepatol* **42**(Suppl 1), S45-S53.

[7] Bajaj JS, Hafeezullah M, Franco J, Varma RR, Hoffmann RG, Knox JF, Hischke D, Hammeke TA, Pinkerton SD, Saeian K (2008) Inhibitory control test for the diagnosis of minimal hepatic encephalopathy. *Gastroenterology* **135**, 1591-1600.e1.

[8] Amodio P, Del Piccolo F, Pettenò E, Mapelli D, Angeli P, Iemmolo R, Muraca M, Musto C, Gerunda G, Rizzo C, Merkel C, Gatta A (2001) Prevalence and prognostic value of quantified electroencephalogram (EEG) alterations in cirrhotic patients. *J Hepatol* **35**, 37-45.

[9] Mullen KD, Prakash RK (2012) Management of covert hepatic encephalopathy. *Clin Liver Dis* **16**, 91-93.

[10] Kappus MR, Bajaj JS (2012) Covert hepatic encephalopathy: Not as minimal as you might think. *Clin Gastroenterol Hepatol* **10**, 1208-1219.

[11] Parsons-Smith BG, Summerskill WH, Dawson AM, Sherlock S (1957) The electroencephalograph in liver disease. *Lancet* **273**, 867-871.

[12] Hawkes CH, Brunt PW (1970) Automatic EEG analysis in hepatic cirrhosis. *Electroencephalogr Clin Neurophysiol* **28**, 428.

[13] Van der Rijt CC, Schalm SW, De Groot GH, De Vlieger M (1984) Objective measurement of hepatic encephalopathy by means of automated EEG analysis. *Electroencephalogr Clin Neurophysiol* **57**, 423-426.

[14] Amodio P, Quero JC, Del Piccolo F, Gatta A, Schalm SW (1996) Diagnostic tools for the detection of subclinical hepatic encephalopathy: Comparison of standard and computerized psychometric tests with spectral-EEG. *Metab Brain Dis* **11**, 315-327.

[15] Amodio P, Marchetti P, Del Piccolo F, de Tourtchaninoff M, Varghese P, Zuliani C, Campo G, Gatta A, Guérit JM (1999) Spectral versus visual EEG analysis in mild hepatic encephalopathy. *Clin Neurophysiol* **110**, 1334-1344.

[16] Amodio P, Pellegrini A, Ubiali E, Mathy I, Piccolo FD, Orsato R, Gatta A, Guerit JM (2006) The EEG assessment of low-grade hepatic encephalopathy: Comparison of an artificial neural network-expert system (ANNES) based evaluation with visual EEG readings and EEG spectral analysis. *Clin Neurophysiol* **117**, 2243-2251.

[17] Amodio P, Orsato R, Marchetti P, Schiff S, Poci C, Angeli P, Gatta A, Sparacino G, Toffolo GM (2009) Electroencephalographic analysis for the assessment of hepatic encephalopathy: Comparison of non-parametric and parametric spectral estimation techniques. *Neurophysiol Clin* **39**, 107-115.

[18] Kullmann F, Hollerbach S, Lock G, Holstege A, Dierks T, Schölmerich J (2001) Brain electrical activity mapping of EEG for the diagnosis of (sub)clinical hepatic encephalopathy in chronic liver disease. *Eur J Gastroenterol Hepatol* **13**, 513-522.

[19] Sun QJ, Wang AH, Zhu MJ, Han J, Zhang XQ (2007) EEG, CT and MRI findings in hepatic encephalopathy. *Nan Fang Yi Ke Da Xue Xue Bao* **27**, 1759-1761.

[20] Marchetti P, D'Avanzo C, Orsato R, Montagnese S, Schiff S, Kaplan PW, Piccione F, Merkel C, Gatta A, Sparacino G, Toffolo GM, Amodio P (2011) Electroencephalography in patients with cirrhosis. *Gastroenterology* **141**, 1680-9e1-e2.

[21] Quero JC, Hartmann IJ, Meulstee J, Hop WC, Schalm SW (1996) The diagnosis of subclinical hepatic encephalopathy in patients with cirrhosis using neuropsychological tests and automated electroencephalogram analysis. *Hepatology* **24**, 556-560.

[22] Olesen SS, Graversen C, Hansen TM, Blauenfeldt RA, Hansen JB, Steimle K, Drewes AM (2011) Spectral and dynamic electroencephalogram abnormalities are correlated to psychometric test performance in hepatic encephalopathy. *Scand J Gastroenterol* **46**, 988-996.

[23] Sagalés T, Gimeno V, de la Calzada MD, Casellas F, Dolors MM, Villar SM (1990) Brain mapping analysis in patients with hepatic encephalopathy. *Brain Topogr* **2**, 221-228.

[24] Hori T (1985) Spatiotemporal changes of EEG activity during wakingsleeping transition period. *Int J Neurosci* **27**, 101-114.

[25] Santamaria J, Chiappa KH (1987) The EEG of drowsiness in normal adults. *J Clin Neurophysiol* **4**, 327-382.

[26] De Gennaro L, Vecchio F, Ferrara M, Curcio G, Rossini PM, Babiloni C (2004) Changes in fronto-posterior functional coupling at sleep onset in humans. *J Sleep Res* **13**, 209-217.

[27] Montagnese S, Jackson C, Morgan MY (2007) Spatio-temporal decomposition of the electroencephalogram in patients with cirrhosis. *J Hepatol* **46**, 447-458.

[28] Amodio P, Marchetti P, Del Piccolo F, Rizzo C, Iemmolo RM, Caregaro L, Gerunda G, Gatta A (1998) Study on the Sternberg paradigm in cirrhotic patients without overt hepatic encephalopathy. *Metab Brain Dis* **13**, 159-172.

[29] Babiloni C, Binetti G, Cassetta E, Cerboneschi D, Dal Forno G, Del Percio C, Ferreri F, Ferri R, Lanuzza B, Miniussi C, Moretti DV, Nobili F, Pascual-Marqui RD, Rodriguez G, Romani GL, Salinari S, Tecchio F, Vitali P, Zanetti O, Zappasodi F, Rossini PM (2004) Mapping distributed sources of cortical rhythms in mild Alzheimer's disease. A multicentric EEG study. *NeuroImage* **22**, 57-67.

[30] Babiloni C, Binetti G, Cassetta E, Dal Forno G, Del Percio C, Ferreri F, Ferri R, Frisoni G, Hirata K, Lanuzza B, Miniussi C, Moretti DV, Nobili F, Rodriguez G, Romani GL, Salinari S, Rossini PM (2006) Sources of cortical rhythms change as a function of cognitive impairment in pathological aging: A multicenter study. *Clin Neurophysiol* **117**, 252-268.

[31] Babiloni C, Cassetta E, Binetti G, Tombini M, Del Percio C, Ferreri F, Ferri R, Frisoni G, Lanuzza B, Nobili F, Parisi L, Rodriguez G, Frigerio L, Gurzì M, Prestia A, Vernieri F, Eusebi F, Rossini PM (2007) Resting EEG sources correlate with attentional span in mild cognitive impairment and Alzheimer's disease. *Eur J Neurosci* **25**, 3742-3757.

[32] Babiloni C, Squitti R, Del Percio C, Cassetta E, Ventriglia MC, Ferreri F, Tombini M, Frisoni G, Binetti G, Gurzi M, Salinari S, Zappasodi F, Rossini PM (2007) Free copper and resting temporal EEG rhythms correlate across healthy, mild cognitive impairment, and Alzheimer's disease subjects. *Clin Neurophysiol* **118**, 1244-1260.

[33] Dierks T, Jelic V, Pascual-Marqui RD, Wahlund LO, Julin P, Linden DEJ, Maurer K, Winblad B, Nordberg A (2000) Spatial pattern of cerebral glucose metabolism (PET) correlates with localization of intracerebral EEG-generators in Alzheimer's disease. *Clin Neurophysiol* **111**, 1817-1824.

[34] Huang C, Wahlund LO, Dierks T, Julin P, Winblad B, Jelic V (2000) Discrimination of Alzheimer's disease and mild cognitive impairment by equivalent EEG sources: A cross-sectional and longitudinal study. *Clin Neurophysiol* **11**, 1961-1967.

[35] Babiloni C, De Pandis MF, Vecchio F, Buffo P, Sorpresi F, Frisoni GB, Rossini PM (2011) Cortical sources of resting state electroencephalographic rhythms in Parkinson's

disease related dementia and Alzheimer's disease. *Clin Neurophysiol* **122**, 2355-2364.
[36] During EH, Osorio RS, Elahi FM, Mosconi L, de Leon MJ (2011) The concept of FDG-PET endophenotype in Alzheimer's disease. *Neurol Sci* **32**, 559-569.
[37] Jones EA, Mullen KD (2012) Theories of the pathogenesis of hepatic encephalopathy. *Clin Liver Dis* **16**, 7-26.
[38] Schomerus H, Hamster W (1998) Neuropsychological aspects of portal-systemic encephalopathy. *Metab Brain Dis* **13**, 361-377.
[39] Weissenborn K, Ennen JC, Schomerus H, Rückert N, Hecker H (2001) Neuropsychological characterization of hepatic encephalopathy. *J Hepatol* **34**, 768-773.
[40] Amodio P, Campagna F, Olianas S, Iannizzi P, Mapelli D, Penzo M, Angeli P, Gatta A (2008) Detection of minimal hepatic encephalopathy: Normalization and optimization of the Psychometric Hepatic Encephalopathy Score. A neuropsychological and quantified EEG study. *J Hepatol* **49**, 346-353.
[41] Petersen RC, Smith GE, Ivnik RJ, Tangalos EG, Schaid SN, Thibodeau SN, Kokmen E, Waring SC, Kurland LT (1995) Apolipoprotein E status as a predictor of the development of Alzheimer's disease in memory-impaired individuals. *JAMA* **273**, 1274-1278.
[42] Petersen RC, Doody R, Kurz A, Mohs RC, Morris JC, Rabins PV, Ritchie K, Rossor M, Thal L, Winblad B (2001) Current concepts in mild cognitive impairment. *Arch Neurol* **58**, 1985-1992.
[43] Grundman M, Petersen RC, Ferris SH, Thomas RG, Aisen PS, Bennett DA, Foster NL, Jack CR Jr, Galasko DR, Doody R, Kaye J, Sano M, Mohs R, Gauthier S, Kim HT, Jin S, Schultz AN, Schafer K, Mulnard R, van Dyck CH, Mintzer J, Zamrini EY, Cahn-Weiner D, Thal LJ; Alzheimer's Disease Cooperative Study (2004) Mild cognitive impairment can be distinguished from Alzheimer disease and normal aging for clinical trials. *Arch Neurol* **61**, 59-66.
[44] McKhann G, Drachman D, Folstein M, Katzman R, Price D, Stadlan EM (1984) Clinical diagnosis of Alzheimer's disease: Report of the NINCDS-ADRDA Work Group under the auspices of Department of Health and Human Services Task Force on Alzheimer's disease. *Neurology* **34**, 939-944.
[45] Rosen WG, Terry RD, Fuld PA, Katzman R, Peck A (1980) Pathological verification of ischemic score in differentiation of dementias. *Ann Neurol* **7**, 486-488.
[46] Yesavage JA, Brink TL, Rose TL, Lum O, Huang V, Adey M, Leirer VO (1982-83) Development and validation of a geriatric depression screening scale: A preliminary report. *J Psychiatr Res* **17**, 37-49.
[47] Folstein MF, Folstein SE, McHugh PR (1975) 'Mini Mental State': A practical method for grading the cognitive state of patients for clinician. *J Psychiat Res* **12**, 189-198.
[48] Lawton MP, Brodie EM (1969) Assessment of older people: Self maintaining and instrumental activity of daily living. *J Gerontol* **9**, 179-186.
[49] Román GC, Tatemichi TK, Erkinjuntti T, Cummings JL, Masdeu JC, Garcia JH, Amaducci L, Orgogozo JM, Brun A, Hofman A et al. (1993) Vascular dementia: Diagnostic criteria for research studies Report of the NINDS-AIREN International Workshop. *Neurology* **43**, 250-260.
[50] McKeith IG, Dickson DW, Lowe J, Emre M, O'Brien JT, Feldman H, Cummings J, Duda JE, Lippa C, Perry EK, Aarsland D, Arai H, Ballard CG, Boeve B, Burn DJ, Costa D, Del Ser T, Dubois B, Galasko D, Gauthier S, Goetz CG, Gomez-Tortosa E, Halliday G, Hansen LA, Hardy J, Iwatsubo T, Kalaria RN, Kaufer D, Kenny RA, Korczyn A, Kosaka K, Lee VM, Lees A, Litvan I, Londos E, Lopez OL, Minoshima S, Mizuno Y, Molina JA, Mukaetova-Ladinska EB, Pasquier F, Perry RH, Schulz JB, Trojanowski JQ, Yamada M (2005) Diagnosis and management of dementia with Lewy bodies: Third report of the DLB Consortium. *Neurology* **65**, 1863-1872.
[51] Moretti DV, Babiloni F, Carducci F, Cincotti F, Remondini E, Rossini PM, Salinari S, Babiloni C (2003) Computerized processing of EEG-EOG-EMG artifacts for multicentric studies in EEG oscillations and event-related potentials. *Int J Psychophysiol* **47**, 199-216.
[52] Besthorn C, Zerfass R, Geiger-Kabisch C, Sattel H, Daniel S, Schreiter-Gasser U, Forstl H (1997) Discrimination of Alzheimer's disease and normal aging by EEG data. *Electroencephalogr Clin Neurophysiol* **103**, 241-248.
[53] Chiaramonti R, Muscas GC, Paganini M, Muller TJ, Fallgatter AJ, Versari A, Strik WK (1997) Correlations of topographical EEG features with clinical severity in mild and moderate dementia of Alzheimer type. *Neuropsychobiology* **36**, 153-158.
[54] Jelic V, Shigeta M, Julin P (1996) Quantitative electroencephalography power and coherence in Alzheimer's disease and mild cognitive impairment. *Dementia* **7**, 314-323.
[55] Leuchter AF, Cook IA, Newton TF, Dunkin J, Walter DO, Rosenberg Tompson S, Lachenbruch PA, Weiner H (1993) Regional differences in brain electrical activity in dementia: Use of spectral power and spectral ratio measures. *Electroenceph Clin Neurophysiol* **87**, 385-393.
[56] Rodriguez G, Copello F, Nobili F, Vitali P, Perego G, Nobili F (1999) EEG spectral profile to stage Alzheimer's disease. *Clin Neurophysiol* **110**, 1831-1837.
[57] Babiloni C, Benussi L, Binetti G, Cassetta E, Dal Forno G, Del Percio C, Ferreri F, Ferri R, Frisoni G, Ghidoni R, Miniussi C, Rodriguez G, Romani GL, Squitti R, Ventriglia MC, Rossini PM (2006) Apolipoprotein E and alpha brain rhythms in mild cognitive impairment: A multicentric Electroencephalogram study. *Ann Neurol* **59**, 323-334.
[58] Babiloni C, Benussi L, Binetti G, Bosco P, Busonero G, Cesaretti S, Dal Forno G, Del Percio C, Ferri R, Frisoni G, Ghidoni R, Rodriguez G, Squitti R, Rossini PM (2006) Genotype (cystatin C) and EEG phenotype in Alzheimer disease and mild cognitive impairment: A multicentric study. *Neuroimage* **29**, 948-964.
[59] Babiloni C, Frisoni G, Steriade M, Bresciani L, Binetti G, Del Percio C, Geroldi C, Miniussi C, Nobili F, Rodriguez G, Zappasodi F, Carfagna T, Rossini PM (2006) Frontal white matter volume and delta EEG sources negatively correlate in awake subjects with mild cognitive impairment and Alzheimer's disease. *Clin Neurophysiol* **117**, 1113-1129.
[60] Babiloni C, Cassetta E, Dal Forno G, Del Percio C, Ferreri F, Ferri R, Lanuzza B, Miniussi C, Moretti DV, Nobili F, Pascual-Marqui RD, Rodriguez G, Luca Romani G, Salinari S, Zanetti O, Rossini PM (2006) Donepezil effects on sources of cortical rhythms in mild Alzheimer's disease: Responders vs. Non-Responders. *Neuroimage* **31**, 1650-1665.
[61] Babiloni C, Vecchio F, Cappa S, Pasqualetti P, Rossi S, Miniussi C, Rossini PM (2006) Functional frontoparietal connectivity during encoding and retrieval processes follows HERA model. A high-resolution study. *Brain Res Bull* **68**, 203-212.
[62] Babiloni C, Bosco P, Ghidoni R, Del Percio C, Squitti R, Binetti G, Benussi L, Ferri R, Frisoni G, Lanuzza B, Cassetta E, Anello G, Gurzi M, Bartesaghi S, Lizio R, Tombini M, Rossini PM (2007) Homocysteine and

electroencephalographic rhythms in Alzheimer disease: A multicentric study. *Neuroscience* **145**, 942-954.

[63] Babiloni C, Frisoni GB, Pievani M, Vecchio F, Infarinato F, Geroldi C, Salinari S, Ferri R, Fracassi C, Eusebi F, Rossini PM (2008) White matter vascular lesions are related to parietal-to-frontal coupling of EEG rhythms in mild cognitive impairment. *Hum Brain Mapp* **29**, 1355-1367.

[64] Babiloni C, Frisoni GB, Pievani M, Toscano L, Del Percio C, Geroldi C, Eusebi F, Miniussi C, Rossini PM (2008) White-matter vascular lesions correlate with alpha EEG sources in mild cognitive impairment. *Neuropsychologia* **46**, 1707-1720.

[65] Babiloni C, Frisoni GB, Pievani M, Vecchio F, Lizio R, Buttiglione M, Geroldi C, Fracassi C, Eusebi F, Ferri R, Rossini PM (2009) Hippocampal volume and cortical sources of EEG alpha rhythms in mild cognitive impairment and Alzheimer disease. *Neuroimage* **44**, 123-135.

[66] Babiloni C, Pievani M, Vecchio F, Geroldi C, Eusebi F, Fracassi C, Fletcher E, De Carli C, Boccardi M, Rossini PM, Frisoni GB (2009) White-matter lesions along the cholinergic tracts are related to cortical sources of EEG rhythms in amnesic mild cognitive impairment. *Hum Brain Mapp* **30**, 1431-1443.

[67] Babiloni C, Frisoni GB, Vecchio F, Pievani M, Geroldi C, De Carli C, Ferri R, Vernieri F, Lizio R, Rossini PM (2010) Global functional coupling of resting EEG rhythms is related to white-matter lesions along the cholinergic tracts in subjects with amnesic mild cognitive impairment. *J Alzheimers Dis* **19**, 859-871.

[68] Babiloni C, Visser PJ, Frisoni G, De Deyn PP, Bresciani L, Jelic V, Nagels G, Rodriguez G, Rossini PM, Vecchio F, Colombo D, Verhey F, Wahlund LO, Nobili F (2010) Cortical sources of resting EEG rhythms in mild cognitive impairment and subjective memory complaint. *Neurobiol Aging* **31**, 1787-1798.

[69] Babiloni C, Frisoni GB, Vecchio F, Lizio R, Pievani M, Cristina G, Fracassi C, Vernieri F, Rodriguez G, Nobili F, Ferri R, Rossini PM (2011) Stability of clinical condition in mild cognitive impairment is related to cortical sources of alpha rhythms: An electroencephalographic study. *Hum Brain Mapp* **32**, 1916-1931.

[70] Babiloni C, Lizio R, Carducci F, Vecchio F, Redolfi A, Marino S, Tedeschi G, Montella P, Guizzaro A, Esposito F, Bozzao A, Giubilei F, Orzi F, Quattrocchi CC, Soricelli A, Salvatore E, Baglieri A, Bramanti P, Cavedo E, Ferri R, Cosentino F, Ferrara M, Mundi C, Grilli G, Pugliese S, Gerardi G, Parisi L, Vernieri F, Triggiani AI, Pedersen JT, Hårdemark HG, Rossini PM, Frisoni GB (2011) Resting state cortical electroencephalographic rhythms and white matter vascular lesions in subjects with Alzheimer's disease: An Italian multicenter study. *J Alzheimers Dis* **26**, 331-346.

[71] Babiloni C, Carducci F, Lizio R, Vecchio F, Baglieri A, Bernardini S, Cavedo E, Bozzao A, Buttinelli C, Esposito F, Giubilei F, Guizzaro A, Marino S, Montella P, Quattrocchi CC, Redolfi A, Soricelli A, Tedeschi G, Ferri R, Rossi-Fedele G, Ursini F, Scrascia F, Vernieri F, Pedersen TJ, Hardemark HG, Rossini PM, Frisoni GB (2012) Resting state cortical electroencephalographic rhythms are related to gray matter volume in subjects with mild cognitive impairment and Alzheimer's disease. *Hum Brain Mapp*, doi: 10.1002/hbm.22005

[72] Holschneider DP, Waite JJ, Leuchter AF, Walton NY, Scremin OU (1999) Changes in electrocortical power and coherence in response to the selective cholinergic immunotoxin 192 IgG-saporin. *Exp Brain Res* **126**, 270-280.

[73] Kolev V, Yordanova J, Basar-Eroglu C, Basar E (2002) Age effects on visual EEG responses reveal distinct frontal alpha networks. *Clin Neurophysiol* **113**, 901-910.

[74] Nobili F, Taddei G, Vitali P, Bazzano L, Catsafados E, Mariani G, Rodriguez G (1998) Relationships between 99m Tc-HMPAO ceraspect and quantitative EEG observations in Alzheimer's disease. *Arch Gerontol Geriatr* **6**, 363-368.

[75] Pucci E, Cacchiò G, Angeloni R, Belardinelli N, Nolfe G, Signorino M, Angeleri F (1997) EEG spectral analysis Alzheimer's disease and different degenerative dementias. *Arch Gereontol Geriatr* **26**, 283-297.

[76] Klimesch W (1996) Memory processes, brain oscillations and EEG synchronization. *Int J Psychophysiol* **24**, 61-100.

[77] Klimesch W (1999) EEG alpha and theta oscillations reflect cognitive and memory performance: A review and analysis. *Brain Res Rev* **29**, 169-195.

[78] Klimesch W, Doppelmayr M, Pachinger T, Russegger H (1997) Event-related desynchronization in the alpha band and the processing of semantic information. *Brain Res Cogn Brain Res* **6**, 83-94.

[79] Klimesch W, Doppelmayr M, Russegger H, Pachinger T, Schwaiger J (1998) Induced alpha band power changes in the human EEG and attention. *Neurosci Lett* **244**, 73-76.

[80] Pascual-Marqui RD, Michel CM (1994) LORETA (low resolution brain electromagnetic tomography): New authentic 3D functional images of the brain. *ISBET Newsletter ISSN* **5**, 4-8.

[81] Pascual-Marqui RD, Lehmann D, Koenig T, Kochi K, Merlo MC, Hell D, Koukkou M (1999) Low resolution brain electromagnetic tomography (LORETA) functional imaging in acute, neuroleptic-naive, first-episode, productive schizophrenia. *Psychiatry Res* **90**, 169-179.

[82] Pascual-Marqui RD, Esslen M, Kochi K, Lehmann D (2002) Functional imaging with low resolution brain electromagnetic tomography (LORETA): A review. *Meth Findings Exp Clin Pharmacol* **24**, 91-95.

[83] Phillips C, Rugg MD, Friston KJ (2002) Systemic regularization of linear inverse solutions of the EEG source localization problem. *Neuroimage* **17**, 287-301.

[84] Yao D, He B (2001) A self-coherence enhancement algorithm and its application to enhancing three-dimensional source estimation from EEGs. *Ann Biomed Eng* **29**, 1019-1027.

[85] Talairach J, Tournoux P (1988) *Co-Planar Stereotaxic Atlas of the Human Brain*. Thieme, Stuttgart.

[86] Anderer P, Saletu B, Semlitsch HV, Pascual-Marqui RD (2003) Non-invasive localization of P300 sources in normal aging and age-associated memory impairment. *Neurobiol Aging* **24**, 463-479.

[87] Anderer P, Saletu B, Saletu-Zyhlarz G, Gruber D, Metka M, Huber J, Pascual-Marqui RD (2004) Brain regions activated during an auditory discrimination task in insomniac postmenopausal patients before and after hormone replacement therapy: Low-resolution brain electromagnetic tomography applied to event-related potentials. *Neuropsychobiology* **49**, 134-153.

[88] Laufer I, Pratt H (2003) Evoked potentials to auditory movement sensation in duplex perception. *Clin Neurophysiol* **114**, 1316-1331.

[89] Mulert C, Gallinat J, Pascual-Marqui R, Dorn H, Frick K, Schlattmann P, Mientus S, Herrmann WM, Winterer G (2001) Reduced event-related current density in the anterior cingulate cortex in schizophrenia. *Neuroimage* **13**, 589-600.

[90] Gerloff C, Richard J, Hadley J, Schulman AE, Honda M, Hallett M (1998) Functional coupling and regional activa-

tion of human cortical motor areas during simple, internally paced and externally paced finger movements. *Brain* **121**, 1513-1531.

[91] Thatcher RW, Krause PJ, Hrybyk M (1986) Cortico-cortical associations and EEG coherence: A two-compartmental model. *Electroencephalogr Clin Neurophysiol* **64**, 123-143.

[92] Rappelsberger P, Petsche H (1988) Probability mapping: Power and coherence analyses of cognitive processes. *Brain Topogr Fall* **1**, 46-54.

[93] Gevins A, Smith ME, Leong H, McEvoy L, Whitfield S, Du R, Rush G (1998) Monitoring working memory load during computer-based tasks with EEG pattern recognition methods. *Hum Factors* **40**, 79-91.

[94] Locatelli T, Cursi M, Liberati D, Franceschi M, Comi G (1998) EEG coherence in Alzheimer's disease. *Electroencephalogr Clin Neurophysiol* **106**, 229-237.

[95] Halliday DM, Rosenberg JR, Amjad AM, Breeze P, Conway BA, Farmer SF (1995) A framework for the analysis of mixed time series/point process data—theory and application to the study of physiological tremor, single motor unit discharges and electromyograms. *Prog Biophys Mol Biol* **64**, 237-278.

[96] Babiloni C, Brancucci A, Vecchio F, Arendt-Nielsen L, Chen AC, Rossini PM (2006) Anticipation of somatosensory and motor events increases centro-parietal functional coupling: An EEG coherence study. *Clin Neurophysiol* **117**, 1000-1008.

[97] Babiloni C, Frisoni GB, Vecchio F, Pievani M, Geroldi C, De Carli C, Ferri R, Vernieri F, Lizio R, Rossini PM (2010) Global functional coupling of resting EEG rhythms is related to white-matter lesions along the cholinergic tracts in subjects with amnesic mild cognitive impairment. *J Alzheimers Dis* **19**, 859-871.

[98] Babiloni C, Vecchio F, Lizio R, Ferri R, Rodriguez G, Marzano N, Frisoni GB, Rossini PM (2011) Resting state cortical rhythms in mild cognitive impairment and Alzheimer's disease: Electroencephalographic evidence. *J Alzheimers Dis* **26**(Suppl 3), 201-214.

[99] Del Percio C, Iacoboni M, Lizio R, Marzano N, Infarinato F, Vecchio F, Bertollo M, Robazza C, Comani S, Limatola C, Babiloni C (2011) Functional coupling of parietal α rhythms is enhanced in athletes before visuomotor performance: A coherence electroencephalographic study. *Neuroscience* **175**, 198-211.

[100] Rossini PM, Del Percio C, Pasqualetti P, Cassetta E, Binetti G, Dal Forno G, Ferreri F, Frisoni G, Chiovenda P, Miniussi C, Parisi L, Tombini M, Vecchio F, Babiloni C (2006) Conversion from mild cognitive impairment to Alzheimer's disease is predicted by sources and coherence of brain electroencephalography rhythms. *Neuroscience* **143**, 793-803.

[101] Vecchio F, Babiloni C, Ferreri F, Curcio G, Fini R, Del Percio C, Rossini PM (2007) Mobile phone emission modulates interhemispheric functional coupling of EEG alpha rhythms. *Eur J Neurosci* **25**, 1908-1913.

[102] Vecchio F, Babiloni C, Ferreri F, Buffo P, Cibelli G, Curcio G, van Dijkman S, Melgari JM, Giambattistelli F, Rossini PM (2010) Mobile phone emission modulates interhemispheric functional coupling of EEG alpha rhythms in elderly compared to young subjects. *Clin Neurophysiol* **121**, 163-171.

[103] Steriade M, Llinás RR (1988) The functional states of the thalamus and the associated neuronal interplay. *Physiol Rev* **68**, 649-742.

[104] Killiany RJ, Moss MB, Albert MS, Sandor T, Tieman J, Jolesz F (1993) Temporal lobe regions on magnetic resonance imaging identify patients with early Alzheimer's disease. *Arch Neurol* **50**, 949-954.

[105] Steriade M, Amzica F, Contreras D (1994) Cortical and thalamic cellular correlates of electroencephalographic burst-suppression. *Electroencephalogr Clin Neurophysiol* **90**, 1-16.

[106] Niedermeyer E (1997) Alpha rhythms as physiological and abnormal phenomena. *Int J Psychophysiol* **26**, 31-49.

[107] Fernández A, Arrazola J, Maestú F, Amo C, Gil-Gregorio P, Wienbruch C, Ortiz T (2003) Correlations of hippocampal atrophy and focal low-frequency magnetic activity in Alzheimer disease: Volumetric MR imaging-magnetoencephalographic study. *AJNR Am J Neuroradiol* **24**, 481-487.

[108] Nobili F, Cutolo M, Sulli A, Castaldi A, Sardanelli F, Accardo S, Rosadini G, Rodriguez G (1997) Impaired quantitative cerebral blood flow in scleroderma patients. *J Neurol Sci* **152**, 63-71.

[109] Moeller JJ, Tu B, Bazil CW (2011) Quantitative and qualitative analysis of ambulatory electroencephalography during mild traumatic brain injury. *Arch Neurol* **68**, 1595-1598.

[110] Vernon PA (1993) *Biological Approaches to the Study of Human Intelligence*. Ablex, Norwood, NJ.

[111] Haier RJ, Siegel BV, Nuechterlein KH, Hazlett E, Wu JC, Paek J, Browning HL, Buchsbaum MS (1988) Cortical glucose metabolicrate correlates of abstract reasoning and attention studied with positron emission tomography. *Intelligence* **12**, 199-217.

[112] Haier RJ, Jung RE, Yeo RA, Head K, Alkire MT (2004) Structural brain variation and general intelligence. *NeuroImage* **23**, 425-433.

[113] Rypma B, Berger JS, Prabhakaran V, Bly BM, Kimberg DY, Biswal BB, D'Esposito M (2006) Neural correlates of cognitive efficiency. *NeuroImage* **33**, 969-979.

[114] Limon A, Reyes-Ruiz JM, Miledi R (2011) GABAergic drugs and Alzheimer's disease. *Future Med Chem* **3**, 149-153.

[115] Ahboucha S, Butterworth RF (2004) Pathophysiology of hepatic encephalopathy: A new look at GABA from the molecular standpoint. *Metab Brain Dis* **19**, 331-343.

[116] Palomero-Gallagher N, Bidmon HJ, Cremer M, Schleicher A, Kircheis G, Reifenberger G, Kostopoulos G, Häussinger D, Zilles K (2009) Neurotransmitter receptor imbalances in motor cortex and basal ganglia in hepatic encephalopathy. *Cell Physiol Biochem* **24**, 291-306.

[117] Ahboucha S, Butterworth RF (2007) The neurosteroid system: An emerging therapeutic target for hepatic encephalopathy. *Metab Brain Dis* **22**, 291-308.

[118] Cauli O, Llansola M, Erceg S, Felipo V (2006) Hypolocomotion in rats with chronic liver failure is due to increased glutamate and activation of metabotropic glutamate receptors in substantia nigra. *J Hepatol* **45**, 654-661.

[119] Ferreri F, Pauri F, Pasqualetti P, Fini R, Dal Forno G, Rossini PM (2003) Motor cortex excitability in Alzheimer's disease: A transcranial magnetic stimulation study. *Ann Neurol* **53**, 102-108.

[120] Di Lazzaro V, Oliviero A, Pilato F, Saturno E, Dileone M, Marra C, Daniele A, Ghirlanda S, Gainotti G, Tonali PA (2004) Motor cortex hyperexcitability to transcranial magnetic stimulation in Alzheimer's disease. *J Neurol Neurosurg Psychiatry* **75**, 555-559.

[121] Butterworth RF (1996) The neurobiology of hepatic encephalopathy. *Semin Liver Dis* **16**, 235-244.

[122] Felipo V, Butterworth RF (2002) Neurobiology of ammonia. *Prog Neurobiol* **67**, 259-279.